nature genetics

Common variants at *SCN5A-SCN10A* and *HEY2* are associated with Brugada syndrome, a rare disease with high risk of sudden cardiac death

Connie R Bezzina[1,44], Julien Barc[1,2,44], Yuka Mizusawa[1,44], Carol Ann Remme[1,44], Jean-Baptiste Gourraud[3–6,44], Floriane Simonet[3–5], Arie O Verkerk[7], Peter J Schwartz[8–13], Lia Crotti[8,9,14], Federica Dagradi[8,9], Pascale Guicheney[15,16], Véronique Fressart[15–17], Antoine Leenhardt[18–20], Charles Antzelevitch[21], Susan Bartkowiak[21], Eric Schulze-Bahr[22], Sven Zumhagen[22], Elijah R Behr[23], Rachel Bastiaenen[23], Jacob Tfelt-Hansen[24,25], Morten Salling Olesen[24,25], Stefan Kääb[26,27], Britt M Beckmann[26], Peter Weeke[28], Hiroshi Watanabe[29], Naoto Endo[30], Tohru Minamino[29], Minoru Horie[31], Seiko Ohno[31], Kanae Hasegawa[31], Naomasa Makita[32], Akihiko Nogami[33], Wataru Shimizu[34,35], Takeshi Aiba[35], Philippe Froguel[36–38], Beverley Balkau[39,40], Olivier Lantieri[41], Margherita Torchio[8,9], Cornelia Wiese[42], David Weber[42], Rianne Wolswinkel[1], Ruben Coronel[1], Bas J Boukens[1,7], Stéphane Bézieau[43], Eric Charpentier[3–5], Stéphanie Chatel[3–6], Aurore Despres[3–6], Françoise Gros[3–5], Florence Kyndt[3–6,43], Simon Lecointe[3–6], Pierre Lindenbaum[3–6], Vincent Portero[3–5], Jade Violleau[3–6], Manfred Gessler[42], Hanno L Tan[1], Dan M Roden[28], Vincent M Christoffels[7], Hervé Le Marec[3–6], Arthur A Wilde[1,44], Vincent Probst[3–6,44], Jean-Jacques Schott[3–6,44], Christian Dina[3–6,44] & Richard Redon[3–6,44]

Brugada syndrome is a rare cardiac arrhythmia disorder, causally related to *SCN5A* mutations in around 20% of cases[1–3]. Through a genome-wide association study of 312 individuals with Brugada syndrome and 1,115 controls, we detected 2 significant association signals at the *SCN10A* locus (rs10428132) and near the *HEY2* gene (rs9388451). Independent replication confirmed both signals (meta-analyses: rs10428132, $P = 1.0 \times 10^{-68}$; rs9388451, $P = 5.1 \times 10^{-17}$) and identified one additional signal in *SCN5A* (at 3p21; rs11708996, $P = 1.0 \times 10^{-14}$). The cumulative effect of the three loci on disease susceptibility was unexpectedly large ($P_{trend} = 6.1 \times 10^{-81}$). The association signals at *SCN5A-SCN10A* demonstrate that genetic polymorphisms modulating cardiac conduction[4–7] can also influence susceptibility to cardiac arrhythmia. The implication of association with *HEY2*, supported by new evidence that Hey2 regulates cardiac electrical activity, shows that Brugada syndrome may originate from altered transcriptional programming during cardiac development[8]. Altogether, our findings indicate that common genetic variation can have a strong impact on the predisposition to rare diseases.

Sudden cardiac death (SCD) is a leading cause of mortality in Western countries, with an incidence close to 1 per 1,000 individuals per year[9]. SCD results most frequently from ventricular fibrillation in the setting of coronary artery disease[10]. In 5–10% of cases, however, SCD occurs owing to rare inherited cardiac arrhythmias, which are typically associated with a distinctive electrocardiogram (ECG) pattern in the absence of identifiable structural heart disease[10]. One such disorder is Brugada syndrome, characterized by ST-segment elevation in right precordial ECG leads[2]. ST-segment elevation may be transient in nature and can be evoked by pharmacological sodium channel blockade. Loss-of-function mutations in *SCN5A*, encoding the pore-forming subunit of the cardiac sodium channel ($Na_v1.5$) at 3p21, have been causally related to the disease in ~20% of cases[3,11]. However, whether arrhythmias arise as a result of abnormal conduction, repolarization or both is under debate[12]. Mutations in genes other than *SCN5A* have been found in a small subset of cases, but their involvement in Brugada syndrome remains unclear[13].

Although Brugada syndrome is commonly considered a mendelian disorder with autosomal dominant transmission, studies in families harboring *SCN5A* mutations have demonstrated low disease penetrance[14,15] and, in some instances, absence of the familial *SCN5A* mutation in some affected family members[15]. Also, many cases are sporadic[16,17], and familial linkage analyses have largely been unsuccessful in uncovering new disease-causing genes. These observations suggest a more complex inheritance model. Identifying new genetic risk factors could assist in further diagnosis, provide new insights into underlying molecular mechanisms and yield new information relevant to the broader problem of SCD.

We conducted a genome-wide association study (GWAS) to explore the role of common genetic variants in susceptibility to

*A full list of author affiliations appears at the end of the paper.

Received 18 January; accepted 28 June; published online 21 July 2013; doi:10.1038/ng.2712

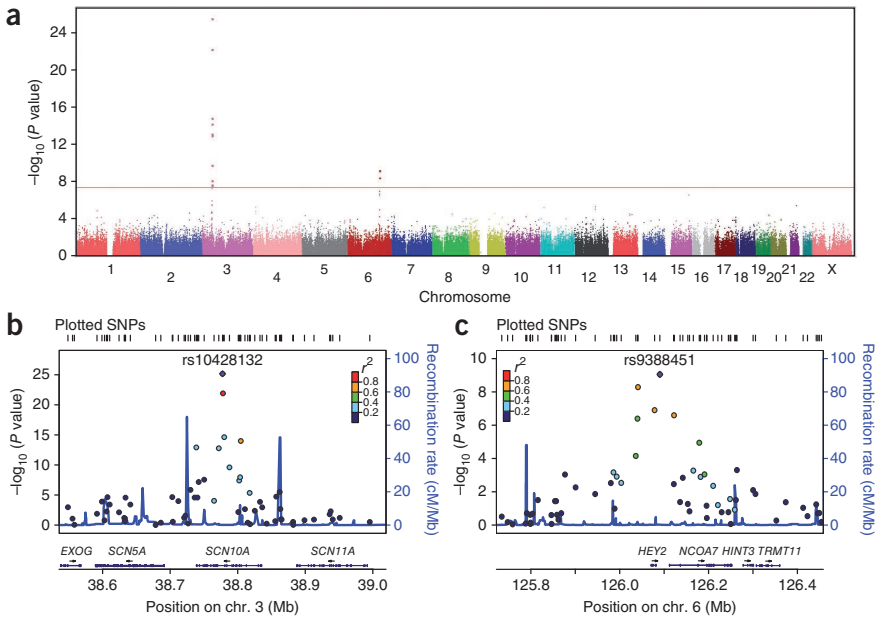

Figure 1 Genome-wide association analysis identifies two susceptibility loci for Brugada syndrome. (**a**) Manhattan plot showing the association of SNPs with Brugada syndrome in a GWAS of 312 cases and 1,115 controls. The red horizontal line marks the threshold for genome-wide significance ($P = 5 \times 10^{-8}$). Two loci reached genome-wide significance on chromosomes 3 and 6. (**b**) Association plots for 3q22 (left) and 6q22 (right). Each SNP is plotted with respect to its chromosomal location (*x* axis) and its association *P* value (left *y* axis). SNPs are colored according to their degree of LD (r^2) with the leading variant represented by a purple diamond and labeled. The tall blue spikes indicate the recombination rate (right *y* axis) in that region of the chromosome. Coordinates are given according to NCBI Build 37.

Brugada syndrome. We established an international consortium enabling the recruitment of 1,114 unrelated, clinically well-defined cases from 13 centers in Europe, the United States and Japan (**Supplementary Table 1**). Every case had a Brugada syndrome type I ECG, as defined by consensus criteria, either at baseline or after drug challenge[2], and *SCN5A* mutation status was systematically assessed.

We first conducted a GWAS on 383 cases of self-reported European ancestry and 898 control individuals from western France (cohort Données Epidémiologiques sur le Syndrome d'Insulino-Résistance (D.E.S.I.R.)[18]). Cases and controls were genotyped using Axiom Genome-Wide CEU 1 arrays (Affymetrix). After stringent quality control and the exclusion of rare SNPs, a total of 360,149 markers were available for further analysis (Online Methods). Multidimensional scaling on the combined cases and controls together with reference populations from the 1000 Genomes Project excluded 42 samples of non-European descent (**Supplementary Fig. 1**). Because controls were largely French individuals, whereas cases had a broader geographic origin, we supplemented the control set with individuals from four European populations from the 1000 Genomes Project that best matched the subsets of cases (**Supplementary Fig. 2**). After the exclusion of 29 cases for whom no matching controls were available, 2 homogeneous groups were defined. GWAS analysis was conducted separately on each group, and association data were combined in a meta-analysis, which included in total 312 cases and 1,115 controls (Online Methods).

We found an excess of SNPs to be associated with Brugada syndrome compared to the number expected under the null hypothesis of no association (**Supplementary Fig. 3**). Two genomic regions showed association signals reaching genome-wide significance (**Fig. 1a**). The most significant association was obtained for rs10428132, a SNP located in the *SCN10A* gene at 3p22 ($P = 6.79 \times 10^{-26}$; **Table 1**). Nine other markers in linkage disequilibrium (LD) with rs10428132 (r^2 = 0.20–0.76) also had associations that reached genome-wide significance (**Fig. 1b** and **Supplementary Table 2**). We detected another cluster of two SNPs in high LD ($r^2 = 0.81$) at 6q22. The lead SNP at this locus was rs9388451 ($P = 8.85 \times 10^{-10}$), located downstream of the *HEY2* gene (**Fig. 1c** and **Supplementary Table 2**). Neither conditional analysis at each associated locus nor GWAS following genome-wide imputation of non-genotyped SNPs uncovered any additional independent association signals at genome-wide significance (Online Methods and **Supplementary Fig. 4**). We confirmed both associations with similar effect sizes when the GWAS was restricted to 856 D.E.S.I.R. controls and 254 ancestry-matched cases by applying stringent exclusion criteria on the multidimensional scaling results (**Supplementary Fig. 5**).

We next considered candidate SNPs identified in previous GWAS on ECG traits[4–7,19–23], using both genotype and imputation data (**Supplementary Table 3**). After the removal of redundant SNPs from the same haplotype ($r^2 > 0.2$) and the exclusion of the haplotype containing rs10428132, we observed a significant enrichment in association for the remaining 54 markers ($P = 5.0 \times 10^{-8}$; **Supplementary Fig. 6**). The SNP with the lowest association *P* value, rs11708996 (**Supplementary Table 3**), was located in *SCN5A* and has previously been associated with variability in PR interval and QRS duration[6,7], two ECG parameters that reflect cardiac conduction, a process possibly affected in Brugada syndrome[12]. Although residing next to the strongest association signal at the 3p22 locus, rs11708996 showed no LD with rs10428132 ($r^2 = 0.06$), and its association *P* value in GWAS data remained unchanged in analysis conditioning on rs10428132, thus suggesting that it represents an independent association (data not shown). Considering the established involvement of *SCN5A* in Brugada syndrome, we carried this SNP forward to the validation step of the study. We also considered SNPs at loci harboring the 11 other susceptibility genes[13] but found no enrichment in association at statistically significant levels (genomic inflation factor (λ_{GC}) = 0.98; Online Methods and **Supplementary Fig. 7**).

We sought to replicate the two genome-wide significant signals (rs10428132 and rs9388451) as well as rs11708996 in an independent case-control set of 594 individuals of European descent with Brugada syndrome and 806 previously genotyped D.E.S.I.R. individuals[24] (Online Methods). All three SNPs showed robust association, with a similar direction of effect as seen in the discovery set, and the signal at rs10428132 reached genome-wide statistical significance in the replication set alone (**Table 1**). To seek additional replication and assess associations in other ancestry groups, we tested a third independent case-control set comprising 208 Japanese cases and 1,016 ancestry-matched controls. We again replicated the three associations, with rs10428132 exceeding the genome-wide significance threshold (**Table 1**). Meta-analysis of the discovery and replication sets yielded highly significant association *P* values for all three loci

Table 1 Discovery and replication studies confirm three alleles on chromosomes 3 and 6 are associated with Brugada syndrome

Marker		rs11708996	rs10428132	rs9388451
Genome position (Build 37)		Chr. 3: 38633923	Chr. 3: 38777554	Chr. 6: 126090377
Closest gene(s)		*SCN5A*	*SCN10A*	*HEY2, NCOA7*
Risk allele		C	T	C
Protective allele		G	G	T
GWAS (312 cases and 1,115 controls; European)[a]	RAF[b]	0.23/0.15	0.69/0.41	0.65/0.50
	P	2.70×10^{-5}	6.79×10^{-26}	8.85×10^{-10}
	OR (CI)	1.64 (1.30–2.07)	3.00 (2.45–3.69)	1.83 (1.51–2.22)
Replication 1 (594 cases and 806 controls; European)[a]	RAF[b]	0.23/0.15	0.65/0.42	0.59/0.50
	P	1.10×10^{-7}	1.66×10^{-30}	2.10×10^{-5}
	OR (CI)	1.69 (1.39–2.04)	2.35 (2.03–2.72)	1.39 (1.19–1.61)
Replication 2 (208 cases and 1,016 controls; Japanese)[a]	RAF[b]	0.09/0.04	0.44/0.23	0.72/0.61
	P	5.63×10^{-5}	1.56×10^{-16}	6.70×10^{-6}
	OR (CI)	2.30 (1.53–3.45)	2.56 (2.05–3.19)	1.74 (1.37–2.21)
Meta-analysis	*P*	1.02×10^{-14}	1.01×10^{-68}	5.14×10^{-17}
	OR (CI)	1.73 (1.51–1.99)	2.55 (2.30–2.84)	1.58 (1.42–1.75)
	Heterogeneity	$Q = 2.17$	$Q = 3.68$	$Q = 5.68$
		$P = 0.338$	$P = 0.159$	$P = 0.058$
		$I^2 = 4\%$	$I^2 = 45\%$	$I^2 = 65\%$
Cases with symptoms[c] (416 cases and 2,937 controls; meta-analysis)[a]	*P*	6.88×10^{-8}	1.15×10^{-39}	5.01×10^{-8}
	OR (CI)	1.73 (1.42–2.12)	2.84 (2.43–3.32)	1.55 (1.32–1.81)

[a]Size of case and control sets; sample ancestry. [b]Risk allele frequency (RAF) in cases over controls. [c]Symptoms included ventricular tachycardia, ventricular fibrillation, syncope and near syncope.

(rs10428132, $P = 1.01 \times 10^{-68}$; rs11708996, $P = 1.02 \times 10^{-14}$; rs9388451, $P = 5.14 \times 10^{-17}$), with the corresponding effect sizes ranging from 1.58 to 2.55 (**Table 1**). Effect sizes were similar when the meta-analysis was restricted to symptomatic individuals, with the association for rs10428132 reaching genome-wide statistical significance (**Table 1**).

We next assessed the cumulative effect of the three loci on susceptibility to Brugada syndrome (**Fig. 2a** and **Supplementary Table 4**). We found that disease risk increased consistently with increasing numbers of carried risk alleles ($P_{trend} = 6.1 \times 10^{-81}$), with the estimated odds ratio (OR) reaching 21.5 in the presence of more than four risk alleles versus less than 2 (**Fig. 2b**). Under a multiplicative model, assuming a prevalence of 0.05% for Brugada syndrome[2] and using the ORs and allele frequencies reported in **Table 1**, the sibling relative risk attributable to the three lead SNPs was estimated at $\lambda_S = 1.4$, with the three loci accounting for 7% of the variance in disease susceptibility (Online Methods). The proportion of the phenotypic variance explained by only these three loci, as well as their cumulative effect, are unexpectedly large in comparison to previously reported effects for common genetic variation on susceptibility to common disease[25]. However, as 1.5% of the European population is expected to carry more than four risk alleles (**Supplementary Table 4**), these three polymorphisms are unlikely to by themselves explain the occurrence of Brugada syndrome and are only associated with a low absolute risk for this rare condition. Furthermore, the ORs reported here were calculated using data from case-control collections and thus may overestimate relative risks.

In subsequent analyses comparing SNP allele dosages in subsets of cases, we could not detect any consistent association of risk alleles with symptoms, *SCN5A* mutation status or Brugada syndrome type I ECG at baseline compared to after drug challenge (**Supplementary Table 5**).

Our strongest association (rs10428132) resides in intron 14 of the *SCN10A* gene, located adjacent to *SCN5A* on chromosome 3p21-22. The particular haplotype tagged by this SNP, which also contains a nonsynonymous variant affecting *SCN10A* (rs6795970, $r^2 = 0.97$ with rs10428132), has previously been associated with variability in PR interval and QRS duration in the general population[4–7]. *SCN10A*, which encodes the sodium channel isoform $Na_v1.8$, was originally reported to be highly expressed in nociceptive sensory neurons of the dorsal root ganglia and cranial sensory ganglia[26]. Besides being expressed in cardiac neurons[27], *SCN10A* was also shown in recent studies to be expressed in the working myocardium[4,28] and the specialized conduction system[7,29], indicating a possible role for $Na_v1.8$ in cardiac electrical function. An independent report implicated the rs6801957 SNP ($r^2 = 0.97$ with rs10428132) as a probable causal variant on the associated haplotype[30]. This SNP, which alters a highly conserved nucleotide within a consensus T-box–binding site, affects TBX5- or TBX3-mediated enhancer activity[30] and is thus expected to affect TBX5/TBX3-regulated expression of *SCN5A* and *SCN10A in vivo*[31]. Further studies are required to determine whether the effects of this SNP on conduction and Brugada syndrome are mediated through regulation of *SCN5A*, *SCN10A* or both. The other independent association at 3p21-22 (rs11708996) involved another haplotype previously associated with cardiac conduction[6,7]. For both haplotypes, the PR- and QRS-prolonging allele was associated with disease risk, providing support for the concept that the cardiomyocyte depolarization process has an important role in the pathogenesis of Brugada syndrome[12].

In contrast to both signals at the *SCN5A-SCN10A* locus, to our knowledge, the signal at 6q22 has never been detected by previous GWAS on ECG traits. The corresponding SNP tagged an LD block

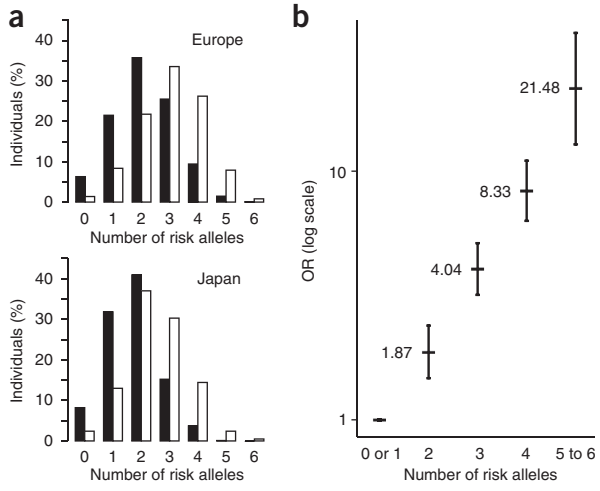

Figure 2 Cumulative effect of alleles at the three associated loci on susceptibility to Brugada syndrome. (**a**) Distribution of risk alleles among individuals with Brugada syndrome (white bars) and among control individuals (black bars) from Europe (top) and Japan (bottom). (**b**) ORs calculated according to the number of risk alleles carried. A meta-analysis was performed as described in the Online Methods, using individuals carrying no or one risk allele as the reference. Each black bar represents the log(OR) value (horizontal bar) and the 95% confidence interval (on the log scale; vertical bar).

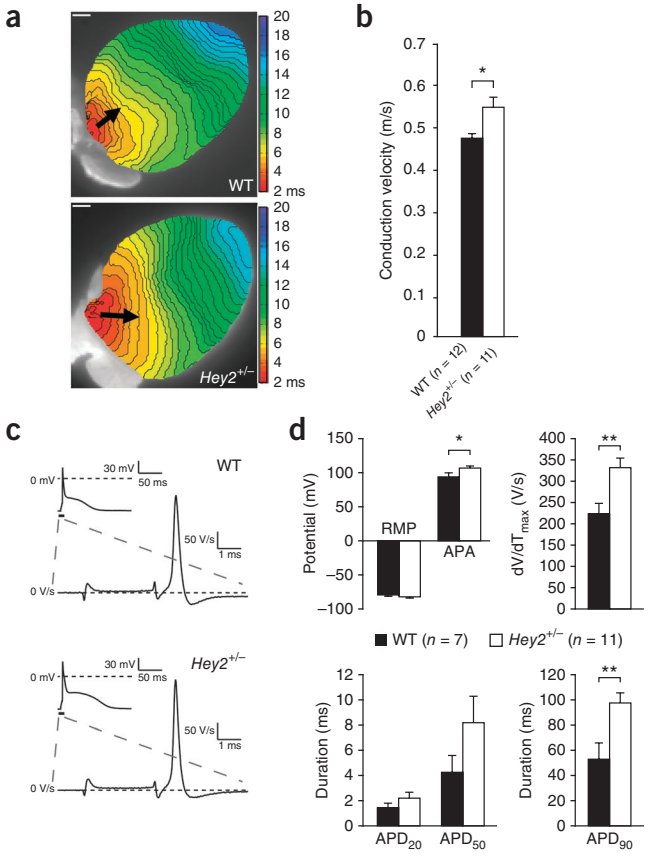

Figure 3 Increased conduction velocity and sodium channel availability in the RVOT of adult *Hey2*$^{+/-}$ mice. (**a**) Representative optical activation maps from isolated wild-type (WT; $n = 12$) and *Hey2*$^{+/-}$ ($n = 11$) hearts stimulated at the RVOT at a basic cycle length of 120 ms (scale bars, 1 mm). Arrows indicate conduction along the RVOT epicardium through the connection of similar isochrones. Isochrones (0.5-ms intervals) in the RVOT of *Hey2*$^{+/-}$ hearts are less crowded compared to wild-type isochromes, indicating faster conduction in the RVOT of *Hey2*$^{+/-}$ hearts (as indicated by increased arrow length). (**b**) On average, conduction velocity in the RVOT of *Hey2*$^{+/-}$ hearts was significantly increased compared to that in wild-type hears ($^{*}P < 0.05$; Student's *t* test). Error bars, s.e.m. (**c**) Representative action potentials measured in adult wild-type (WT; $n = 7$) and *Hey2*$^{+/-}$ ($n = 11$) cardiomyocytes isolated from RVOT. (**d**) Average action potential characteristics measured at 4 Hz. RVOT cardiomyocytes from *Hey2*$^{+/-}$ mice showed a significant increase in maximal upstroke velocity (dV/dT_{max}, a measure of sodium channel availability and a determinant of conduction velocity) and action potential amplitude (APA), indicating increased sodium channel availability ($^{*}P < 0.05$; $^{**}P < 0.01$; Student's *t* test). Resting membrane potential (RMP), action potential duration at 20% and 50% repolarization (APD_{20} and APD_{50}, respectively) were not significantly different in wild-type and *Hey2*$^{+/-}$ mice; action potential duration at 90% repolarization (APD_{90}) was significantly increased in RVOT cardiomyocytes from *Hey2*$^{+/-}$ mice. Results are expressed as mean ± s.e.m.

that entirely encompasses the *HEY2* gene and extends into the first intron of *NCOA7* (also called *ERAP140*), which encodes a nuclear receptor coactivator that interacts with estrogen receptor α to modulate its activity[32]. *NCOA7* is predominantly expressed in the brain[32] and has not been implicated in cardiovascular function. In contrast, *HEY2* (also called *HESR2*, *HRT2* and *CHF1*) encodes a basic helix-loop-helix (bHLH) transcriptional repressor that is expressed in the cardiovascular system[8].

Studies we have conducted in *Hey2*-targeted mice provide strong support for the role of this gene in Brugada syndrome. In the developing mouse heart, *Hey2* expression is confined to the (subepicardial) compact myocardium of the ventricle[33]. *Hey2*-null mice exhibit a spectrum of developmental anomalies, including ventricular wall thinning, abnormal right ventricular morphology and postnatal cardiomyopathic changes[34–37]. The expression of *Gja5* (encoding Cx40), *Nppa* and *Tbx5*, normally enriched in the (subendocardial) trabecular component of the ventricle, is expanded into the compact myocardium in *Hey2*-deficient embryos[34,38,39]. Because such transmural heterogeneity in expression is similarly well established for $Na_v1.5$ (high expression in subendocardium, low expression in subepicardium)[40], loss of *Hey2* might also affect the transmural expression gradient of this ion channel implicated in Brugada syndrome[2,3]. Indeed, in hearts from homozygous *Hey2*-null embryos, we observed higher $Na_v1.5$ expression in the compact layer than in wild-type hearts, flattening the expression gradient of this channel (**Supplementary Fig. 8a**).

The functional consequences of Hey2 loss were investigated in adult heterozygous *Hey2* mice (*Hey2*$^{+/-}$), which have structurally normal hearts (**Supplementary Fig. 9**). *In vivo* surface ECG parameters were unchanged in *Hey2*$^{+/-}$ mice (**Supplementary Fig. 10**). However, conduction velocity was significantly increased in the right ventricular outflow tract (RVOT) of isolated *Hey2*$^{+/-}$ hearts (**Fig. 3a**,**b**), whereas conduction velocity was unaffected in the right and left ventricular free wall (**Supplementary Fig. 11**). Action potential upstroke velocity was increased in *Hey2*$^{+/-}$ myocytes isolated from the RVOT region (**Fig. 3c**,**d**), pointing to increased sodium channel function, despite undetectable changes in $Na_v1.5$ expression in adult hearts from *Hey2*$^{+/-}$ mice in immunohistochemistry analysis (**Supplementary Fig. 8b**). Furthermore, the prolonged repolarization parameters observed in these cells suggest an additional regulatory role for Hey2 in repolarizing currents (**Fig. 3d**). Future work should address whether the observed alterations in action potential characteristics and conduction are mediated through ion channel correlates, subtle structural heart alterations or both. Nevertheless, the preferential involvement of the RVOT is in line with ECG manifestations in right precordial leads and concurs with the observation that the RVOT is a common site of origin of ventricular arrhythmias in individuals with Brugada syndrome[41].

In conclusion, we have identified Hey2 as a transcriptional regulator of cardiac electrical function involved in the pathogenesis of Brugada syndrome. Furthermore, we provide new evidence that common variants, previously shown to modulate ECG conduction indices, also modulate susceptibility to a rare arrhythmia disorder. Most notably, this study demonstrates that the GWAS paradigm can be successfully applied to a rare disorder, previously considered monogenic, to identify common genetic variants with unexpectedly strong modifier effects.

URLs. Affymetrix Power Tools, http://www.affymetrix.com/partners_programs/programs/developer/tools/powertools.affx; GTOOL, http://www.well.ox.ac.uk/~cfreeman/software/gwas/gtool.html; R statistical package, http://www.r-project.org/; 1000 Genomes Project, http://www.1000genomes.org/; 1000 Genomes phase I integrated variant set release, http://mathgen.stats.ox.ac.uk/impute/data_download_1000G_phase1_integrated.html.

METHODS

Methods and any associated references are available in the online version of the paper.

Note: Any Supplementary Information and Source Data files are available in the online version of the paper.

ACKNOWLEDGMENTS

We thank L. Beekman, C. de Gier-de Vries, B. de Jonge and the Genomic Platform of Nantes (Biogenouest Genomics) for technical support. We are also grateful to the French Clinical Network against Inherited Cardiac Arrhythmias, which includes the University Hospitals of Nantes, Bordeaux, Rennes, Tours, Brest, Strasbourg, La Réunion, Angers and Montpellier. This study was funded by research grants from the Leducq Foundation (CVD-05; Alliance Against Sudden Cardiac Death), the Ministry of Education, Culture, Sports, Science and Technology of Japan (grant-in-aid for the Project in Sado for Total Health, PROST), the French Ministry of Health (PHRC AOR04070, P040411 and PHRCI DGS2001/0248), INSERM (ATIP-Avenir program to R.R.) and the French Regional Council of Pays-de-la-Loire. This research was also supported by the Netherlands Heart Institute (grant 061.02 to C.A.R. and C.R.B.) and the Division for Earth and Life Sciences (ALW; project 836.09.003 to C.A.R.) with financial aid from the Netherlands Organization for Scientific Research (NWO). C.R.B. acknowledges support from the Netherlands Heart Foundation (NHS 2007B202 and 2009B066). J.B. was supported by a research grant from the European Society of Cardiology and the Netherlands Heart Institute (ICIN) and by the French-Dutch Academy through the Van Gogh program. E.S.-B. was supported by the Interdisziplinären Zentrums für Klinische Forschung (IZKF) of the University of Münster and the Collaborative Research Center SFB656. M.G. acknowledges support from the German Research Foundation (DFG-SFB 688 and TP A16). This manuscript is dedicated to the memory of Denis Escande, who founded the Leducq Foundation Network Alliance Against Sudden Cardiac Death.

AUTHOR CONTRIBUTIONS

C.R.B., J.-J.S. and R.R. designed the study. Y.M. and J.-B.G. evaluated all ECGs. C.D. coordinated the statistical analyses, which C.D., F.S., P.L. and E.C. carried out. F.G., A.D., S.L. and E.C. performed genotyping for the GWAS. J.B., J.V., V. Portero and K.H. carried out genotyping in the validation sets. A.A.W., H.L.T., H.L.M., V. Probst, F.K., S. Bézieau, S.C., S.K., B.M.B., E.S.-B., S.Z., L.C., P.J.S., F.D., M.T., C.A., S. Bartkowiak, P.G., V.F., A.L., D.M.R., P.W., E.R.B., R.B., J.T.-H., M.S.O., N.M., A.N., M.H., S.O., K.H., W.S. and T.A. recruited subjects and participated in clinical and molecular diagnostics. P.F., B.B., O.L., H.W., T.M. and N.E. provided controls. M.G., D.W. and C.W. provided the mice. C.A.R., A.O.V., B.J.B. and R.W. acquired and analyzed electrophysiological data. V.M.C., C.A.R. and R.W. acquired and analyzed protein expression data. C.R.B., J.B., C.A.R., C.D., J.-J.S., V.M.C., R.C. and R.R. interpreted the data. C.R.B., J.-J.S., V. Probst, D.M.R., A.A.W., S.K., E.S.-B., A.L. and R.R. obtained funding. C.R.B., J.B., C.D. and R.R. drafted the manuscript. All coauthors critically revised the manuscript for intellectual content. C.R.B. and R.R. led the study together.

COMPETING FINANCIAL INTERESTS

The authors declare no competing financial interests.

1. Brugada, P. & Brugada, J. Right bundle branch block, persistent ST segment elevation and sudden cardiac death: a distinct clinical and electrocardiographic syndrome. A multicenter report. *J. Am. Coll. Cardiol.* **20**, 1391–1396 (1992).
2. Antzelevitch, C. *et al.* Brugada syndrome: Report of the Second Consensus Conference Endorsed by the Heart Rhythm Society and the European Heart Rhythm Association. *Circulation* **111**, 659–670 (2005).
3. Kapplinger, J.D. *et al.* An international compendium of mutations in the *SCN5A*-encoded cardiac sodium channel in patients referred for Brugada syndrome genetic testing. *Heart Rhythm* **7**, 33–46 (2010).
4. Chambers, J.C. *et al.* Genetic variation in *SCN10A* influences cardiac conduction. *Nat. Genet.* **42**, 149–152 (2010).
5. Holm, H. *et al.* Several common variants modulate heart rate, PR interval and QRS duration. *Nat. Genet.* **42**, 117–122 (2010).
6. Pfeufer, A. *et al.* Genome-wide association study of PR interval. *Nat. Genet.* **42**, 153–159 (2010).
7. Sotoodehnia, N. *et al.* Common variants in 22 loci are associated with QRS duration and cardiac ventricular conduction. *Nat. Genet.* **42**, 1068–1076 (2010).
8. Leimeister, C., Externbrink, A., Klamt, B. & Gessler, M. *Hey* genes: a novel subfamily of hairy- and Enhancer of split related genes specifically expressed during mouse embryogenesis. *Mech. Dev.* **85**, 173–177 (1999).
9. Straus, S.M.J.M. *et al.* The incidence of sudden cardiac death in the general population. *J. Clin. Epidemiol.* **57**, 98–102 (2004).
10. Priori, S.G. *et al.* Task Force on Sudden Cardiac Death, European Society of Cardiology, Summary of Recommendations. *Europace* **4**, 3–18 (2002).
11. Chen, Q. *et al.* Genetic basis and molecular mechanism for idiopathic ventricular fibrillation. *Nature* **392**, 293–296 (1998).
12. Wilde, A.A.M. *et al.* The pathophysiological mechanism underlying Brugada syndrome: depolarization versus repolarization. *J. Mol. Cell Cardiol.* **49**, 543–553 (2010).
13. Crotti, L. *et al.* Spectrum and prevalence of mutations involving BrS1-through BrS12-susceptibility genes in a cohort of unrelated patients referred for Brugada syndrome genetic testing: implications for genetic testing. *J. Am. Coll. Cardiol.* **60**, 1410–1418 (2012).
14. Priori, S.G. *et al.* Clinical and genetic heterogeneity of right bundle branch block and ST-segment elevation syndrome: a prospective evaluation of 52 families. *Circulation* **102**, 2509–2515 (2000).
15. Probst, V. *et al. SCN5A* mutations and the role of genetic background in the pathophysiology of Brugada syndrome (clinical perspective). *Circ Cardiovasc Genet* **2**, 552–557 (2009).
16. Schulze-Bahr, E. *et al.* Sodium channel gene (*SCN5A*) mutations in 44 index patients with Brugada syndrome: different incidences in familial and sporadic disease. *Hum. Mutat.* **21**, 651–652 (2003).
17. Hermida, J.-S. *et al.* Prospective evaluation of the familial prevalence of the Brugada syndrome. *Am. J. Cardiol.* **106**, 1758–1762 (2010).
18. Balkau, B. An epidemiologic survey from a network of French Health Examination Centres, (D.E.S.I.R.): epidemiologic data on the insulin resistance syndrome. *Rev. Epidemiol. Sante Publique* **44**, 373–375 (1996).
19. Arking, D.E. *et al.* A common genetic variant in the *NOS1* regulator *NOS1AP* modulates cardiac repolarization. *Nat. Genet.* **38**, 644–651 (2006).
20. Newton-Cheh, C. *et al.* Common variants at ten loci influence QT interval duration in the QTGEN Study. *Nat. Genet.* **41**, 399–406 (2009).
21. Pfeufer, A. *et al.* Common variants at ten loci modulate the QT interval duration in the QTSCD Study. *Nat. Genet.* **41**, 407–414 (2009).
22. Eijgelsheim, M. *et al.* Genome-wide association analysis identifies multiple loci related to resting heart rate. *Hum. Mol. Genet.* **19**, 3885–3894 (2010).
23. Marroni, F. *et al.* A genome-wide association scan of RR and QT interval duration in 3 European genetically isolated populations: the EUROSPAN project. *Circ Cardiovasc Genet* **2**, 322–328 (2009).
24. Sladek, R. *et al.* A genome-wide association study identifies novel risk loci for type 2 diabetes. *Nature* **445**, 881–885 (2007).
25. Manolio, T.A. *et al.* Finding the missing heritability of complex diseases. *Nature* **461**, 747–753 (2009).
26. Akopian, A.N., Sivilotti, L. & Wood, J.N. A tetrodotoxin-resistant voltage-gated sodium channel expressed by sensory neurons. *Nature* **379**, 257–262 (1996).
27. Verkerk, A.O. *et al.* Functional Nav1.8 channels in intracardiac neurons: the link between *SCN10A* and cardiac electrophysiology. *Circ. Res.* **111**, 333–343 (2012).
28. Yang, T. *et al.* Blocking Scn10a channels in heart reduces late sodium current and is antiarrhythmic. *Circ. Res.* **111**, 322–332 (2012).
29. Pallante, B.A. *et al.* Contactin-2 expression in the cardiac Purkinje fiber network. *Circ Arrhythm Electrophysiol* **3**, 186–194 (2010).
30. van den Boogaard, M. *et al.* Genetic variation in T-box binding element functionally affects *SCN5A*/*SCN10A* enhancer. *J. Clin. Invest.* **122**, 2519–2530 (2012).
31. Arnolds, D.E. *et al.* TBX5 drives Scn5a expression to regulate cardiac conduction system function. *J. Clin. Invest.* **122**, 2509–2518 (2012).
32. Shao, W., Halachmi, S. & Brown, M. ERAP140, a conserved tissue-specific nuclear receptor coactivator. *Mol. Cell Biol.* **22**, 3358–3372 (2002).
33. Fischer, A. & Gessler, M. *Hey* genes in cardiovascular development. *Trends Cardiovasc. Med.* **13**, 221–226 (2003).
34. Xin, M. *et al.* Essential roles of the bHLH transcription factor Hrt2 in repression of atrial gene expression and maintenance of postnatal cardiac function. *Proc. Natl. Acad. Sci. USA* **104**, 7975–7980 (2007).
35. Kokubo, H. *et al.* Targeted disruption of *hesr2* results in atrioventricular valve anomalies that lead to heart dysfunction. *Circ. Res.* **95**, 540–547 (2004).
36. Gessler, M. *et al.* Mouse gridlock: no aortic coarctation or deficiency, but fatal cardiac defects in *Hey2*$^{-/-}$ mice. *Curr. Biol.* **12**, 1601–1604 (2002).
37. Sakata, Y. *et al.* Ventricular septal defect and cardiomyopathy in mice lacking the transcription factor CHF1/Hey2. *Proc. Natl. Acad. Sci. USA* **99**, 16197–16202 (2002).
38. Koibuchi, N. & Chin, M.T. CHF1/Hey2 plays a pivotal role in left ventricular maturation through suppression of ectopic atrial gene expression. *Circ. Res.* **100**, 850–855 (2007).
39. Fischer, A. *et al.* Hey basic helix-loop-helix transcription factors are repressors of GATA4 and GATA6 and restrict expression of the GATA target gene *ANF* in fetal hearts. *Mol. Cell Biol.* **25**, 8960–8970 (2005).
40. Remme, C.A. *et al.* The cardiac sodium channel displays differential distribution in the conduction system and transmural heterogeneity in the murine ventricular myocardium. *Basic Res. Cardiol.* **104**, 511–522 (2009).
41. Nademanee, K. *et al.* Prevention of ventricular fibrillation episodes in Brugada syndrome by catheter ablation over the anterior right ventricular outflow tract epicardium. *Circulation* **123**, 1270–1279 (2011).

[1]Department of Clinical and Experimental Cardiology, Heart Failure Research Center, Academic Medical Center, Amsterdam, The Netherlands. [2]ICIN (Netherlands Heart Institute), Utrecht, The Netherlands. [3]Institut National de la Santé et de la Recherche Médicale (INSERM) Unité Mixte de Recherche (UMR) 1087, L'Institut du Thorax, Nantes, France. [4]Centre National de la Recherche Scientifique (CNRS) UMR 6291, Nantes, France. [5]Université de Nantes, Nantes, France. [6]Centre Hospitalier Universitaire (CHU) Nantes, L'Institut du Thorax, Service de Cardiologie, Nantes, France. [7]Department of Anatomy, Embryology and Physiology, Heart

Failure Research Center, Academic Medical Center, Amsterdam, The Netherlands. [8]Department of Molecular Medicine, University of Pavia, Pavia, Italy. [9]Center for Cardiac Arrhythmias of Genetic Origin, Istituto di Ricovero e Cura a Carattere Scientifico (IRCCS), Istituto Auxologico Italiano, Milan, Italy. [10]Cardiovascular Genetics Laboratory, Hatter Institute for Cardiovascular Research in Africa, Cape Town, South Africa. [11]Department of Medicine, University of Cape Town, Cape Town, South Africa. [12]Department of Medicine, University of Stellenbosch, Stellenbosch, South Africa. [13]Chair of Sudden Death, Department of Family and Community Medicine, College of Medicine, King Saud University, Riyadh, Saudi Arabia. [14]Institute of Human Genetics, Helmholtz Center Munich, Neuherberg, Germany. [15]INSERM U956, Faculté de Médecine Pierre et Marie Curie, Site Pitié-Salpêtrière, Paris, France. [16]Université Pierre et Marie Curie Université Paris 06, Unité de Mixte Recherche Scientifique (UMRS) 956, Institut Fédératif de Recherche 14, Paris, France. [17]Assistance Publique–Hôpitaux de Paris (AP-HP), Groupe Hospitalier Pitié-Salpétrière, Service de Biochimie Métabolique, Unité Fonctionnelle Cardiogénétique et Myogénétique Moléculaire et Cellulaire, Paris, France. [18]Service de Cardiologie, Centre de Référence des Maladies Cardiaques Héréditaires, Hôpital Bichat, AP-HP, Paris, France. [19]INSERM U698, Paris, France. [20]Université Paris Diderot, Paris, France. [21]Department of Experimental Cardiology, Masonic Medical Research Laboratory, Utica, New York, USA. [22]Institute for Genetics of Heart Diseases (IfGH), Department of Cardiovascular Medicine, University Hospital, Münster, Germany. [23]Cardiovascular Sciences Research Centre, St George's University of London, London, UK. [24]Danish National Research Foundation Centre for Cardiac Arrhythmia (DARC), Laboratory of Molecular Cardiology, University of Copenhagen, Copenhagen, Denmark. [25]Department of Cardiology, The Heart Centre, Copenhagen University Hospital Rigshospitalet, Copenhagen, Denmark. [26]Department of Medicine I, University Hospital Munich, Campus Grosshadern, Ludwig-Maximilians University, Munich, Germany. [27]Deutsches Forschungszentrum für Herz-Kreislauferkrankungen (DZHK), partner site Munich Heart Alliance, Munich, Germany. [28]Department of Medicine and Pharmacology, Vanderbilt University School of Medicine, Nashville, Tennessee, USA. [29]Department of Cardiovascular Biology and Medicine, Niigata University Graduate School of Medical and Dental Sciences, Niigata, Japan. [30]Department of Regenerative and Transplant Medicine, Division of Orthopaedic Surgery, Niigata University Graduate School of Medicine and Dental Science, Niigata, Japan. [31]Department of Cardiovascular and Respiratory Medicine, Shiga University of Medical Science, Otsu, Japan. [32]Department of Molecular Physiology, Graduate School of Biomedical Sciences, Nagasaki University, Nagasaki, Japan. [33]Division of Heart Rhythm Management, Yokohama Rosai Hospital, Yokohama, Japan. [34]Department of Cardiovascular Medicine, Nippon Medical School, Tokyo, Japan. [35]Department of Cardiovascular Medicine, National Cerebral and Cardiovascular Center, Division of Arrhythmia and Electrophysiology, Suita, Japan. [36]CNRS UMR 8199, Lille Pasteur Institute, Lille, France. [37]Lille Nord de France University, Lille, France. [38]Department of Genomics of Common Disease, School of Public Health, Imperial College London, Hammersmith Hospital, London, UK. [39]INSERM U1018, Centre de Recherche en Epidémiologie et Santé des Populations (CESP), Villejuif, France. [40]Université Paris Sud, UMRS 1018, Villejuif, France. [41]Institut Inter-Régional pour la Santé (IRSA), La Riche, France. [42]Developmental Biochemistry, Theodor-Boveri-Institute, Biocenter, University of Würzburg, Würzburg, Germany. [43]CHU Nantes, Service de Génétique Médicale, Nantes, France. [44]These authors contributed equally to this work. Correspondence should be addressed to C.R.B. (c.r.bezzina@amc.uva.nl) or R.R. (richard.redon@inserm.fr).

ONLINE METHODS

Case and control samples. Individuals with Brugada syndrome, defined by the presence of a type 1 ECG[2], were recruited from 13 centers in Europe (Nantes, Paris, Amsterdam, Pavia, Copenhagen, Munich, Münster and London), the United States (Utica and Nashville) and Japan (Nagasaki, Shiga and Osaka). Only index cases were included from extended pedigrees. Appropriate medical ethical committee approval was obtained at each participating clinical center. Informed consent was available from all subjects. Clinical data (age at diagnostic ECG, *SCN5A* mutation status, symptoms and family history of sudden cardiac death) and ECGs were collected centrally and reviewed. A Brugada syndrome type I ECG pattern was defined on the basis of the criteria drawn out at the Second Consensus Conference on Brugada Syndrome[2], namely, a coved type ST elevation at baseline or after a drug challenge test, in one or more leads in the right precordial leads, including the third and fourth intercostal space. Drug challenge tests were performed according to consensus criteria[2]. Control subjects were drawn from the D.E.S.I.R. cohort[18] for the GWAS and the European replication set and were drawn from the Sado study[42] for the Japanese replication set. No statistical method was used to predetermine sample size.

GWAS genotyping. SNP genotyping was performed on population-optimized Affymetrix Axiom Genome-Wide CEU 1 array plates following the standard manufacturer's protocol. Each array contains 567,097 SNPs. Fluorescence intensities were quantified using the Affymetrix GeneTitan Multi-Channel Instrument, and primary analysis was conducted with Affymetrix Power Tools following the manufacturer's recommendations (see URLs). Genotype calling, a two-dimensional clustering analysis, was performed using the 'apt' program. Individuals with genotype call rate of lower than 97% were removed, as were those with fewer than 10,000 markers reporting a heterozygous state (the threshold was determined after visual inspection). Monomorphic SNPs were excluded, as were those with minor allele frequency (MAF) of <10% ($n = 175{,}153$), a call rate of <95% ($n = 19{,}986$) or Hardy-Weinberg disequilibrium in controls ($n = 2{,}054$ with $P < 1 \times 10^{-4}$ when testing for Hardy-Weinberg equilibrium). Note that Hardy-Weinberg disequilibrium was also tested in demographically homogenous cases to identify very large deviations ($P < 1 \times 10^{-7}$). Additional SNPs were excluded for batch effect: such SNPs were defined as those with significant differences in allele frequency in one plate versus all others within cases and within controls only ($n = 68$) or with unexplained large differences observed in controls versus the 1000 Genomes Project European (non-Finnish) population ($n = 9{,}686$).

Demographic analyses. The ancestry of individuals was assessed using a multidimensional scaling technique, as implemented in PLINK[43]. SNPs were selected for short-range LD independence. Pruning was performed using a two-step procedure to accommodate longer range LD (this is particularly important, as the Axiom Human array is enriched in SNPs in the human leukocyte antigen (HLA) region). In a first step, we applied the threshold $r^2 < 0.2$ within a 20-kb LD block or within 50 SNPs. In a second step, we applied the same threshold within a 10-Mb distance or within 100 SNPs on the pruned data set. We then created an identity-by-state (IBS) matrix including all individuals and applied the multidimensional scaling method (–mds option in PLINK) to retrieve the first five components. Three matrices were estimated using our cases and controls together with all 1000 Genomes Project populations (IC) and all European (except Finnish) populations (E). At each level, we excluded outliers on the first two components using an expectation-maximization-fitted Gaussian mixture clustering method[44] implemented in the R package M-CLUST, assuming either three (for IC) or two (for E) clusters and noise. Outlier position was assigned using nearest-neighbor-based classification[45] (NNclust in R package PrabClus). Outliers were excluded from the analysis, as previously done in GWAS[46].

GWAS. Using the clustering algorithm described above, we defined two homogenous groups (A and B). To carry out the genome-wide analysis, each SNP was tested within groups A and B separately, using logistic regression and assuming an additive genetic model with adjustment for the first five components retrieved. No additional covariates were added, as advised[47]. Instead, the results from groups A and B were combined into a meta-analysis using an inverse normal strategy[48], whereby the summary *P* values for each test (and effect direction) are combined into a signed *z* score that, properly weighted, yields $N(\mu = 0, \sigma^2 = 1)$. Because the number of controls exceeded by far the number of cases in all studies, we used the effective sample size (weighting studies A and B) using METAL software as advised[49]. In addition, we performed a second genome-wide analysis on a homogenous sample of 254 cases and 806 controls of apparent French origin (largest geographically homogenous sample; **Supplementary Fig. 5**).

Concordance rate between Axiom and 1000 Genomes Project data. We genotyped 95 HapMap individuals on Affymetrix Axiom Genome-Wide CEU 1 arrays using the same process as described above. We could retrieve the genotypes of 58 of these 95 individuals from the 1000 Genomes Project database. The concordance rate was tested using PLINK (merging mode 7, which compares the common non-missing genotypes). The concordance rate was 99.4% over a total of 20,853,552 genotypes and 100% over the 174 genotypes corresponding to the 3 associated SNPs.

Genome-wide imputation analysis. Genotyped SNPs in cases and controls were phased using the SHAPE-IT (v.1) program[50]. Imputation of 6.1 million frequent SNPs (MAF > 0.05 in Europeans) was carried out using IMPUTE v2 (ref. 51). Chromosome regions were split in chunks of approximately 7 Mb. The reference panel was Phase I integrated variant set release (v3) in NCBI Build 37 (hg19) coordinates (see URLs). For each chromosomal chunk, a set of genetically matched panel individuals was selected, according to the last strategy used by IMPUTE[52]. Imputed SNPs were combined with SNPs extracted from the 1000 Genomes Project data set under the IMPUTE format. We merged both data sets using GTOOL. We applied a logistic regression (additive model) as implemented in SNPTEST[45] (options -frequentist 1 and -score), using the first five components as covariates. Individuals from the 1000 Genomes Project data set were added for all SNPs either genotyped or imputed.

Post-analysis quality control. For each significantly associated SNP in a region (called here lead SNP), we visually inspected the cluster graph (**Supplementary Fig. 12a**) and the association results of SNPs in LD (locus plot).

Enrichment analysis. We tested enrichment in moderately associated SNPs grouped by distinctive properties. The first group included SNPs that have been reported to be associated with ECG traits in previous GWAS. We used the list published in ref. 53 after removal of redundant SNPs (one SNP was selected randomly for each group of SNPs with $r^2 > 0.2$) and exclusion of SNPs located in the same haplotype block as rs10428132. The second list comprised every SNP located within 1-Mb intervals (500 kb upstream and 500 kb downstream) centered on the susceptibility genes for Brugada syndrome listed in ref. 13. We removed the *SCN5A* gene, as it would have disproportionately inflated the overall statistics. Quantile-quantile plots were first visually inspected to check for enrichment. The significance of enrichment suggested by the quantile-quantile plot for the first group (ECG-associated SNPs) was formally tested by a simple Fisher combination test.

Replication genotyping. The three significantly associated SNPs from the GWAS stage (rs10428132, rs9388451 and rs11708996) were typed for the replication steps by TaqMan SNP Genotyping assays (Applied Biosystems) according to the manufacturer's protocol on a LightCycler 480 Real-Time PCR System (Roche) or an ABI Prism 7900HT Sequence Detection System (Applied Biosystems). Assays C__26860683_10, C___2824356_10 and C__44417794_10 were functionally tested by Applied Biosystems for the SNPs rs10428132, rs9388451 and rs11708996, respectively. Reaction conditions included an initial denaturation step at 95 °C for 10 min, followed by 50 cycles of denaturation at 95 °C for 15 s and annealing at 60 °C for 30 s. Data were analyzed with LightCycler 480 software (release 1.5.0 SP4; **Supplementary Fig. 12b**) or by ABI 7900HT Sequence Detection Systems software (**Supplementary Fig. 12c**). Outliers were excluded from the analysis. After the first round of genotyping, two samples per SNP genotype cluster were sequenced to verify genotype (**Supplementary Fig. 12b**). Furthermore, 15 samples that were previously genotyped on Affymetrix Axiom Genome-Wide CEU 1 arrays were used as control samples: the genotypes obtained by TaqMan assays were perfectly concordant with those generated with Axiom array technology.

SNP imputation for the control population used in the European replication. The genotypes of the three SNPs tested in replication were imputed using IMPUTE software for 806 D.E.S.I.R. individuals on the basis of genotype data sets previously generated on Illumina Human CNV370-Duo arrays[24,54]. We selected a threshold of 0.9 for genotype calling, meaning that the genotypes whose posterior probability exceeded this threshold were called, whereas those where this probability was below the threshold were set as unknown. We genotyped 49 individuals on both Affymetrix and Illumina arrays. Once hard calls were obtained using GTOOL (see URLs) with -Gen mode and –threshold option set to 0.9, concordance rates were calculated using PLINK (merging mode 7). Perfect concordance was observed between genotyped and imputed SNPs (100% concordance rate for 144 genotypes).

Replications and meta-analyses. The case-control replication study was performed using a logistic regression method that accounts for genotype calling uncertainty. This method, based on missing data theory, allows the unbiased estimation of ORs and confidence intervals and is implemented in SNPTEST (options–method ml). Pooled ORs were obtained by averaging the ORs from all stages (GWAS and European and Japanese replications) and weighted by the inverse of the variance. Heterogeneity was tested using the Cochran's Q test and was also measured using Higgins' index[55]. We generated genetic scores for individuals on the basis of an allelic scoring system involving our three SNPs. These scores were created either through the number of at-risk alleles for the European discovery and Japanese replication populations or the risk allele dosage in the European replication population. Risk allele dosages from the European replication population were collapsed using dosage. The distribution of imputed dosage is shown in **Supplementary Figure 13a**. Results were similar between imputed dosage ($\beta = 0.62921$, $\sigma = 0.05427$, $P = 4.43 \times 10^{-31}$) and collapsed imputed dosage ($\beta = 0.61778$, $\sigma = 0.05386$, $P = 1.88 \times 10^{-30}$). Moreover, we compared the genetic scores obtained with genotyped versus imputed SNPs for 49 individuals who were genotyped on Axiom Genome-Wide CEU 1 arrays and imputed with the European replication population and observed high correlation between methods (**Supplementary Fig. 13b**). Finally, we tested whether a non-additive model (recessive or dominant) might be a better fit for each genome-wide significant SNP. A heterozygote effect was added to the logistic regression analysis along with the linear effect (effect of the number of alternative alleles) in each study and in a meta-analysis. We did not detect any consistent deviation from the additive model (**Supplementary Table 6**).

Estimation of the genetic score effect by multiple imputation. Despite this high concordance, we chose to estimate genotype score risk within the Multiple Imputation framework[56]. Ten data sets were created where each uncertain genotype was replaced by a value simulated under the probability distribution obtained through genetic imputation (IMPUTE output consisting of P(AA), P(AB) and P(BB)). The β value and variance were obtained using standard procedures[57]. We let m be the number of simulations (called replicates). For each simulation, we carried out a logistic regression (either on score as an ordinal value or on each score versus baseline). The Multiple Imputation effect estimation was calculated as follows:

$$\bar{\beta}_{\mathrm{MI}} = \frac{1}{m}\sum_{j=1}^{m}\beta_j$$

The variance was calculated as the sum of within-replicate and between-replicate variances

$$\sigma^2_{\mathrm{MI}} = \frac{1}{m}\hat{\sigma}^2_j + \frac{1}{m-1}\sum_{j=1}^{m}(\bar{\beta}_{\mathrm{MI}} - \beta_j)^2$$

Confidence intervals were retrieved using the 95% quantile of a Student distribution with a number of degrees of freedom, which is a function of the two components of the variance. We used the 'glm' function of the R statistical package (see URLs) to perform logistic regression. R was used to create complete data sets from IMPUTE output.

Calculation of sibling relative risk and liability-scale variance. Assuming a multiplicative model (within and between variants), the contribution to the sibling relative risk of a set of N SNPs was calculated using the following formula

$$\lambda_s = \prod_{j=1}^{N}\left[1 + \frac{p_j(1-p_j)(\mathrm{OR}_j - 1)^2}{2[(1-p_j) + p_j\mathrm{OR}_j]^2}\right]^2$$

where p_j and OR_j denote the RAF and corresponding allelic OR at the jth SNP[58]. Assuming disease prevalence K, the liability-scale variance[59] explained by these SNPs was calculated as follows:

$$h^2_L = \frac{2[T - T_1\sqrt{1-(T^2 - T_1^2)}(1 - T/\omega)]}{\omega + T_1^2(\omega - T)}$$

In the expression, $T = \varphi^{-1}(1-K)$, $T_1 = \varphi^{-1}(1-\lambda_S K)$ and $\omega = z/K$, where z is the height of the standard Gaussian density at T.

Surface ECG analysis. Mice (male and female, aged 3–5 months) were anesthetized using isoflurane inhalation (0.8–1.0 volume percentage in oxygen), and surface ECGs were recorded from subcutaneous 23-gauge needle electrodes attached to each limb using the Powerlab acquisition system (ADInstruments). ECG traces were signal averaged and analyzed for heart rate (RR interval) and for PR-interval, QRS-interval and QT-interval duration using LabChart7Pro software (ADInstruments). QT intervals were corrected for heart rate using the formula $\mathrm{QTc} = \mathrm{QT}/\sqrt{\mathrm{RR}/100}$ (RR in ms).

Optical mapping in isolated hearts. Mice were anesthetized by an intraperitoneal injection of pentobarbital, after which the heart was excised, cannulated, incubated in 10 ml Tyrode's solution containing 15 μM Di-4 ANEPPS and subsequently placed in an optical mapping setup. Hearts were perfused at 37 °C with Tyrode's solution (128 mM NaCl, 4.7 mM KCl, 1.45 mM $CaCl_2$, 0.6 mM $MgCl_2$, 27 mM $NaHCO_3$, 0.4 mM NaH_2PO_4 and 11 mM glucose (pH maintained at 7.4 by equilibration with a mixture of 95% O_2 and 5% CO_2)) containing blebbistatin to prevent movement artifacts. Excitation light was provided by a 5-W power LED (filtered 510 ± 20 nm). Fluorescence (filtered for >610 nm) was transmitted through a tandem lens system on a CMOS sensor (100 × 100 elements; MICAM Ultima). Hearts were paced at a basic cycle length (BCL) of 120 ms (twice the diastolic stimulation threshold) from the center of the right or left ventricle epicardial surface or from the RVOT epicardial surface. Optical action potentials were analyzed with custom software. Local activation was defined as the maximum positive slope of the action potential, and local activation times were used to construct ventricular activation maps. To calculate conduction velocity in longitudinal and transversal directions in the right and left ventricles, the difference in activation time between at least three consecutive electrode terminals separated by a known distance located parallel (longitudinal) or perpendicular (transversal) to the direction of propagation was measured. The direction of propagation was determined using isochronal maps. For c velocity measurements in the RVOT, transverse fiber direction was defined as the slowest conduction velocity.

Action potential measurements in isolated cardiomyocytes. Cardiomyocytes were isolated by enzymatic dissociation as previously described[60]. After perfusion of the heart with enzyme solution, the RVOT area at the base of the right ventricle just below the truncus pulmonalis was excised and used during the subsequent isolation process[43]. Quiescent rod-shaped cross-striated cells with a smooth surface were selected for measurements. Action potentials were recorded with the amphotericin-B-perforated patch-clamp using an Axopatch 200B Clamp amplifier (Molecular Devices Corporation). Signals were filtered (low pass, 10 kHz) and digitized (40 kHz), and action potentials were corrected for the estimated change in liquid junction potential. Action potentials were measured at 36 ± 0.2 °C using a modified Tyrode's solution containing 140 mM NaCl, 5.4 mM KCl, 1.8 mM $CaCl_2$, 1.0 mM $MgCl_2$, 5.5 mM glucose and 5.0 mM HEPES, pH 7.4 (NaOH). Pipettes (1.5–2.5 MΩ) were filled with solution containing 125 mM potassium gluconate, 20 mM KCl, 10 mM NaCl, 0.22 mM amphotericin-B and 10 mM HEPES, pH 7.2 (KOH). Action potentials were elicited at 4 Hz by 3 ms, 1.2× threshold current pulses

doi:10.1038/ng.2712

through the patch pipette. We analyzed resting membrane potential (RMP), action potential amplitude (APA), maximal upstroke velocity (dV/dt_{max}) and action potential duration at 20, 50 and 90% repolarization (APD_{20}, APD_{50} and APD_{90}, respectively). Data from ten consecutive action potentials were averaged. Results are expressed as mean ± s.e.m. Two sets of data were considered significantly different if the *P* value of the unpaired Student's *t* test with Bonferroni correction was <0.05.

Other methods. Procedures for immunohistochemistry hybridization on mouse heart sections were performed as described previously[40].

42. Sakuma, M. *et al.* Incidence and outcome of osteoporotic fractures in 2004 in Sado City, Niigata Prefecture, Japan. *J. Bone Miner. Metab.* **26**, 373–378 (2008).
43. Purcell, S. *et al.* PLINK: a tool set for whole-genome association and population-based linkage analyses. *Am. J. Hum. Genet.* **81**, 559–575 (2007).
44. Frayley, C. & Raftery, A.E. *MCLUST Version 3 for R: Normal Mixture Modeling and Model-Based Clustering* (Department of Statistics, University of Washington, Seattle, 2006).
45. Byers, S. & Raftery, A.E. Nearest-neighbor clutter removal for estimating features in spatial point processes. *J. Am. Stat. Assoc.* **93**, 577–584 (1998).
46. Postel-Vinay, S. *et al.* Common variants near *TARDBP* and *EGR2* are associated with susceptibility to Ewing sarcoma. *Nat. Genet.* **44**, 323–327 (2012).
47. Pirinen, M., Donnelly, P. & Spencer, C.C.A. Including known covariates can reduce power to detect genetic effects in case-control studies. *Nat. Genet.* **44**, 848–851 (2012).
48. Stouffer, S.A., Suchman, E.A., Devinney, L.C., Star, S.A. & Williams, R.M. Jr. *The American Soldier: Adjustment During Army Life (Studies in Social Psychology in World War II, Vol. 1)* (Princeton University Press, Princeton, NJ, 1949).
49. Willer, C.J., Li, Y. & Abecasis, G.R. METAL: fast and efficient meta-analysis of genomewide association scans. *Bioinformatics* **26**, 2190–2191 (2010).
50. Delaneau, O., Marchini, J. & Zagury, J.-F. A linear complexity phasing method for thousands of genomes. *Nat. Methods* **9**, 179–181 (2012).
51. Marchini, J., Howie, B., Myers, S., McVean, G. & Donnelly, P. A new multipoint method for genome-wide association studies by imputation of genotypes. *Nat. Genet.* **39**, 906–913 (2007).
52. Howie, B., Marchini, J. & Stephens, M. Genotype imputation with thousands of genomes. *G3* **1**, 457–470 (2011).
53. Kolder, I.C.R.M., Tanck, M.W.T. & Bezzina, C.R. Common genetic variation modulating cardiac ECG parameters and susceptibility to sudden cardiac death. *J. Mol. Cell Cardiol.* **52**, 620–629 (2012).
54. Meyre, D. *et al.* Genome-wide association study for early-onset and morbid adult obesity identifies three new risk loci in European populations. *Nat. Genet.* **41**, 157–159 (2009).
55. Higgins, J.P.T. & Thompson, S.G. Quantifying heterogeneity in a meta-analysis. *Stat. Med.* **21**, 1539–1558 (2002).
56. Little, R.J.A. & Rubin, D.B. *Statistical Analysis with Missing Data* (Wiley and Sons, New York, 1987).
57. Rubin, D.B. *Multiple Imputation for Nonresponse in Surveys* (2008) http://onlinelibrary.wiley.com/book/10.1002/9780470316696.
58. Lin, S., Chakravarti, A. & Cutler, D.J. Exhaustive allelic transmission disequilibrium tests as a new approach to genome-wide association studies. *Nat. Genet.* **36**, 1181–1188 (2004).
59. Wray, N.R., Yang, J., Goddard, M.E. & Visscher, P.M. The genetic interpretation of area under the ROC curve in genomic profiling. *PLoS Genet.* **6**, e1000864 (2010).
60. Remme, C.A. *et al.* Overlap syndrome of cardiac sodium channel disease in mice carrying the equivalent mutation of human *SCN5A*-1795insD. *Circulation* **114**, 2584–2594 (2006).